5. J. M. Schnur, *Science* **262**, 1669 (1993); C. A. Huber *et al.*, *ibid.* **263**, 800 (1994); G. M. Whitesides, J. P. Mathias, C. T. Seto, *ibid.* **254**, 1312 (1991).
6. C. D. Bain and G. M. Whitesides, *Angew. Chem. Int. Ed. Engl.* **28**, 506 (1989); A. Ulman, *An Introduction to Ultrathin Organic Films, from Langmuir-Blodgett to Self-Assembly* (Academic Press, Boston, 1991).
7. K. C. Grabar, R. G. Freeman, M. B. Hommer, M. J. Natan, *Anal. Chem.*, in press.
8. K. C. Grabar *et al.*, in preparation.
9. P. Matejka, B. Vlcková, J. Vohlidal, P. Pancoska, V. Baumruk, *J. Phys. Chem.* **96**, 1361 (1992); P. C. Lee and D. Meisel, *Chem. Phys. Lett.* **99**, 262 (1983).
10. C. Bohren and D. R. Huffman, *Absorption and Scattering of Light by Small Particles* (Wiley, New York, 1983).
11. K. C. Grabar *et al.*, in preparation.
12. P. X. Zhang, Y. Fang, W. N. Wang, D. H. Ni, S. Y. Fu, *J. Raman Spectrosc.* **21**, 127 (1990); J. Wiesner and A. Wokaun, *Chem. Phys. Lett.* **157**, 569 (1989); C. G. Blatchford, J. R. Campbell, J. A. Creighton, *Surf. Sci.* **120**, 435 (1982).
13. The AFM image from a glass slide coated with 3-aminopropylmethyldimethoxysilane indicates an overall roughness of 1 to 3 nm, notwithstanding a few isolated locations where the polymer roughness approaches 8 to 10 nm. This roughness scale is typical for organosilane films on glass or quartz (*20*). Immobilization of 12-nm colloidal Au particles to a coverage equivalent to that shown for 180 to 210 min in Fig. 2A yields a surface with features 12 to 20 nm high and 20 to 30 nm wide. The increased dispersion in particle size relative to TEM results from convolution of the true particle size with the AFM tip size (*21*) but is nevertheless of sufficient quality to indicate that the surface is composed of a monolayer of separated particles, in agreement with FE-SEM images on similar substrates.
14. D. L. Jeanmaire and R. P. Van Duyne, *J. Electroanal. Chem.* **84**, 1 (1977).
15. C. Amatore, J. M. Savéant, D. Tessier, *ibid.* **147**, 39 (1983).
16. A. E. G. Cass, Ed., *Biosensors: A Practical Approach* (Oxford Univ. Press, Oxford, 1990).
17. The optical constants for Au and Ag were taken from R. H. Morriss and L. F. Collins [*J. Chem. Phys.* **41**, 3357 (1961)]. These values were fit to exponential curves to generate continuous values between 300 and 700 nm.
18. We calculated an enhancement factor (EF) of 5.7×10^5 for the Ag-coated surface by comparing the ratios of background-corrected intensities for a SERS spectrum and a solution spectrum in units of counts per second per watt per molecule, and averaging the EF values obtained for six different common peaks. A low signal-to-noise ratio precluded calculation of accurate EFs for the as-prepared Au sample.
19. E. J. Zeman and G. C. Schatz, *J. Phys. Chem.* **91**, 634 (1987); M. Inoue and K. Ohtaka, *J. Phys. Soc. Jpn.* **52**, 3853 (1983); L.-C. Chu and S.-Y. Wang, *J. Appl. Phys.* **57**, 453 (1985); *Phys. Rev. B* **31**, 693 (1985).
20. S. Karrasch, M. Dolder, F. Schabert, J. Ramsden, A. Engel, *Biophys. J.* **65**, 2437 (1993); W. J. Dressick, C. S. Dulcey, J. H. Georger Jr., G. S. Calabrese, J. M. Calvert, *J. Electrochem. Soc.* **141**, 210 (1994).
21. D. Keller, *Surf. Sci.* **253**, 353 (1991).
22. G. Frens, *Nature Phys. Sci.* **241**, 20 (1973); W. S. Sutherland and J. D. Winefordner, *J. Colloid Interface Sci.* **48**, 129 (1992).
23. P. C. Lee and D. Meisel, *J. Phys. Chem.* **86**, 3391 (1982).
24. This research was supported in part by the Petroleum Research Fund (25694-G5) administered by the American Chemical Society, the Beckman Young Investigator Program, and The Pennsylvania State University (PSU). The National Science Foundation (CHE-9300292) provided an undergraduate fellowship to M.B.H., the Particulate Materials Center at PSU furnished an undergraduate fellowship to P.C.S., and Eastman Kodak Company underwrote for a graduate fellowship to K.C.G. We thank PPG Industries for a gift of SnO_2, the Electron Microscopy Facility for the Life Sciences in the Biotechnology Institute at PSU, and C. T. Bohren for the computer programs BHMIE and BHCOAT.

20 September 1994; accepted 29 December 1994

Granular Convection Observed by Magnetic Resonance Imaging

E. E. Ehrichs, H. M. Jaeger,* Greg S. Karczmar, James B. Knight, Vadim Yu. Kuperman, Sidney R. Nagel

Vibrations in a granular material can spontaneously produce convection rolls reminiscent of those seen in fluids. Magnetic resonance imaging provides a sensitive and noninvasive probe for the detection of these convection currents, which have otherwise been difficult to observe. A magnetic resonance imaging study of convection in a column of poppy seeds yielded data about the detailed shape of the convection rolls and the depth dependence of the convection velocity. The velocity was found to decrease exponentially with depth; a simple model for this behavior is presented here.

More than a century ago, Faraday discovered that vibration can produce large-scale convection within a granular medium (*1*). Like molecules of a liquid heated from below, grains in a vibrating container continuously circulate between the bottom and top of the container. This ubiquitous phenomenon has implications for a wide variety of industrial processes, but the mechanisms that cause it are poorly understood even today (*2*). One unusual and perplexing feature is that the grains flow rapidly at the container walls rather than exhibiting the nonslip boundary condition observed in normal fluids. Investigators have been hampered by an inability to see motion deep inside a container so as to determine the full, three-dimensional convection pattern. Here, we report a noninvasive convection measurement technique that provides the detailed shape of the boundary layer and the functional form of the convection velocity.

Much effort in the past has focused on calculations of flow patterns and velocity profiles in industrially important situations such as chute flow and discharge from hoppers (*3–5*). More recently, large-scale computer simulations have been used to model convection (*6, 7*) and size separation (*8, 9*) in vibrated granular materials, but few experimental data on the interior of the granular flow are available for comparison with these models. In two-dimensional geometries, particles can be tracked optically (*10–12*); however, because such experiments necessitate front and back walls and their associated friction, it is unclear how these results relate to the more technologically relevant three-dimensional case, where granular convection can be a driving mechanism for size segregation (*13*) and where optical tracking is difficult. Early three-dimensional experiments used invasive methods in which the granular aggregate was cast in resin and cross sections were cut and examined (*14*). Noninvasive techniques using x-rays (*15*) and radioactive tracer particles (*16*) also have been explored, but neither approach has yet resulted in a high-resolution tool for the study of granular flow.

Magnetic resonance imaging (MRI) offers a promising alternative for visualizing convection flows. With this technique it is possible to image arbitrary cross sections through the interior of a granular aggregate and to obtain direct information about the velocity profiles. Altobelli *et al.* (*17*) have used MRI to study particles in liquid suspensions, and Nakagawa *et al.* (*18*) have used MRI to study the flow of dry granular materials in a rotating drum. In the latter study, the use of oil-containing seeds as the granular material provided sufficient free protons in the liquid state to produce an acceptable signal-to-noise ratio. Here, we use this technique to study convection rolls induced by vertical vibrations in a column of white poppy seeds.

A magnetic resonance image of the poppy seeds at rest in a small cylindrical glass container is shown in Fig. 1. As in (*18*), a single layer of seeds was glued to the inner surface of the container. This coating makes the walls of the container visible in the image, thus giving a base line from which to measure the vertical displacement of the seeds, and it also provides a controlled degree of friction between the walls and the vibrating seeds (*13*). Inside the bore of the MRI magnet,

E. E. Ehrichs, H. M. Jaeger, J. B. Knight, S. R. Nagel, James Franck Institute and Department of Physics, University of Chicago, 5640 South Ellis Avenue, Chicago, IL 60637, USA.
G. S. Karczmar and V. Yu. Kuperman, Department of Radiology, University of Chicago, Chicago, IL 60637, USA.

*To whom correspondence should be addressed.

a nonmetallic sample platform vertically accelerated the container of seeds. The vibration was driven by a VG100 vibration exciter (Vibration Test Systems) that was located approximately 3 m from the magnet. Vibrations were coupled from the exciter to the platform through rotary motion transmitted by a rigid rod. A cam beneath the platform converted back-and-forth rotary motion around the central axis of the rod into vertical up-and-down shakes. Typically, individual, well-separated shakes were applied. Acceleration of the platform was measured with an accelerometer (PCB Piezotronics 353B01). To induce convection, an applied acceleration, Γ, greater than Earth's acceleration $g = 9.8$ m s^{-2} was required (*13, 19–21*).

An unresolved problem is to determine the detailed spatial shape and the depth dependence of the interior flow profile for a granular convection roll (*6, 7, 13*). MRI enables investigators to address these questions by tagging well-defined regions of the grains and observing their evolution with shaking. Here, we chose to tag seeds selectively in a horizontal stripe pattern so that we could extract information about vertical displacements. The seeds were tagged by modulating the longitudinal spin polarization throughout the sample (*22*) in the vertical direction (Fig. 2A). After a single shake, individual seeds have moved, carrying with them the spin modulation and creating a distortion of the originally horizontal stripes (Fig. 2B). The stripes near the top have clearly bent but remain well defined; this pattern implies collective flow of the granular material. The material in the center has moved up while the material along the edges has moved down. The stripes close to the bottom of the container stayed relatively straight and unperturbed after one shake; this observation indicates that net motion decreases with increasing depth from the surface.

Images such as Fig. 2B can be processed digitally (*23*) to extract data about the vertical seed displacement after one shake, that is, the convection velocity. The processed data (Fig. 3, A and B) demonstrate the high accuracy with which the grain displacement can be determined. The largest displacement, and thus the highest convection velocity, occurs near the walls in the downward-moving portion of the roll. This boundary region is only one to two seed diameters wide (Fig. 3B); this finding is the first direct experimental determination of this width in a three-dimensional geometry. The high resolution provided by MRI allows us to observe deviations from a straight, plug-flow, profile in the upward-moving central portion of the flow. This flow appears to become more pluglike as the ratio of container diameter to grain size is increased (*24*).

The dependence of the upward velocity, v_u, as a function of depth, z, along the central axis of the container is shown (Fig. 4) for several values of the acceleration.

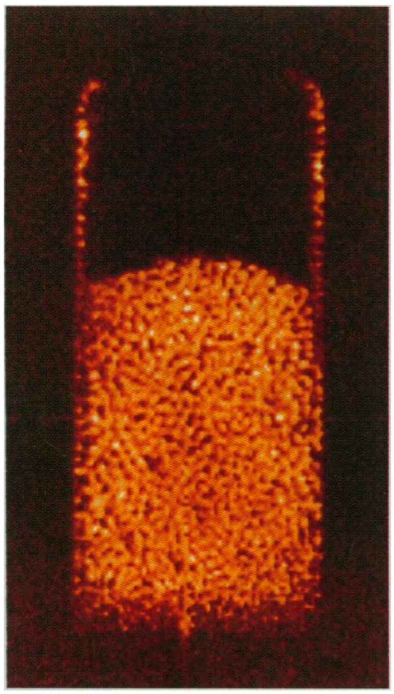

Fig. 1. Magnetic resonance image of a 1-mm slice through the center of a glass cylinder containing white poppy seeds (color is arbitrary). Each grain visible in the image is an individual seed. The seeds are smooth and slightly oblong with an average major axis of 1 mm. They were sifted to select a range of minor axes from 0.7 to 0.8 mm. The average mass of each seed is 380 μg. The inside diameter of the container is 16.5 mm and the height of the column of seeds is 27 mm. The coating of seeds glued to the inner surface of the container is visible on the side walls above the top surface of the seeds. All images were obtained by means of a 2.0 Tesla GE/Bruker machine with a CSI operating system.

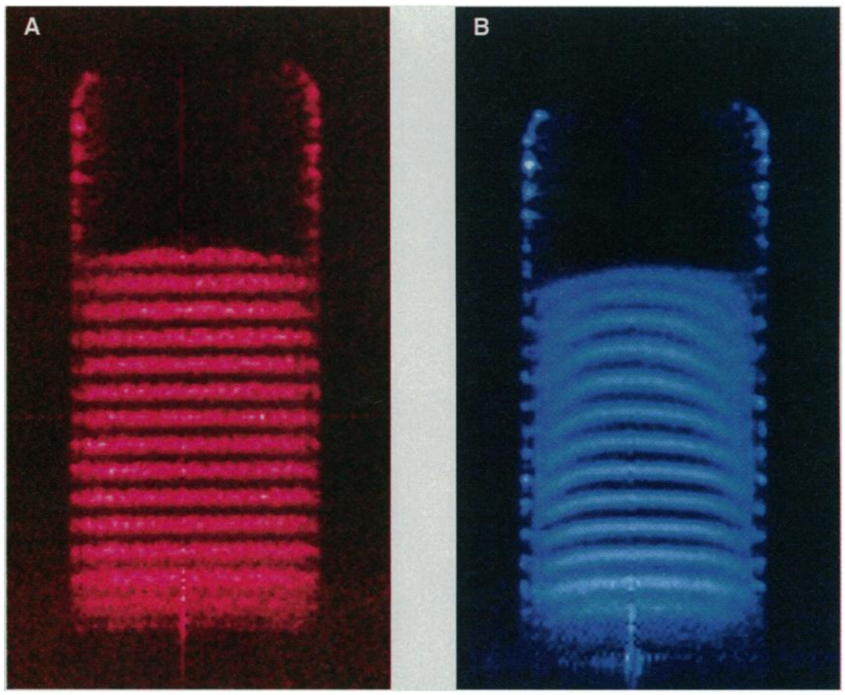

Fig. 2. (**A**) Image of a 2-mm slice through the center of the container shown in Fig. 1. A sequence of magnetic field gradients and radio frequency pulses was used to prepare the system with a sinusoidally varying nuclear spin polarization, giving rise to a longitudinal magnetization $M_{\ell}(z,t) = M_0[\cos(\mathbf{k}_z z) - 1] \exp(-t/T_1) + M_0$, where M_0 is the equilibrium magnetization in the magnetic field, z is the vertical coordinate along the axis of the container (the direction of the applied magnetic field is perpendicular to z), t is the elapsed time, $\mathbf{k}_z$ is the wave vector of the modulation, and the spin-lattice relaxation time T_1 (which for white poppy seeds is about 200 ms at 2 T) is the time constant for the exponential decay of the modulation. T_1 sets the time frame within which shaking of the container and subsequent image collection must occur. The peaks of the modulation appear as bright stripes in the image and are used to label narrow regions in the granular material. (**B**) Magnetic resonance image of the system prepared in the same way as in (A) but after a single shake of peak acceleration $\Gamma = 8g$. To extract the information to produce one complete image, separate phase-encoded gradient echoes (*31*) from 256 identical shakes were required. The result shown here is the average of eight such images. The crispness of the image (assembled from 2048 separate shakes) attests to the repeatability of the shakes. Each shake consists of a single 20-Hz sinusoidal period of acceleration. The system is then allowed to come to rest for 0.7 s before subsequent shaking; this step eliminates any effects from incomplete relaxation between pulses. The phenomena are robust to the details of the applied shake. The layer of seeds glued to the wall provides a marker for the position of the stripes before the shake.

With the exception of the uppermost region, the data in Fig. 4 are well accounted for by an exponential dependence of v_u below the top surface, of the form

$$v_u(z) = v_u(0)\exp(-z/\xi) \quad (1)$$

where ξ is a decay length. We have found that the length scale, ξ, depends not only on the value of the applied acceleration, Γ, but also on the peak displacement during the shake pulse. Such an exponential dependence of v_u suggests a constant depth-independent probability for particles being scattered near the walls from the downward-moving flow, j_d, into the central, upward-moving flow, j_u, expressed by

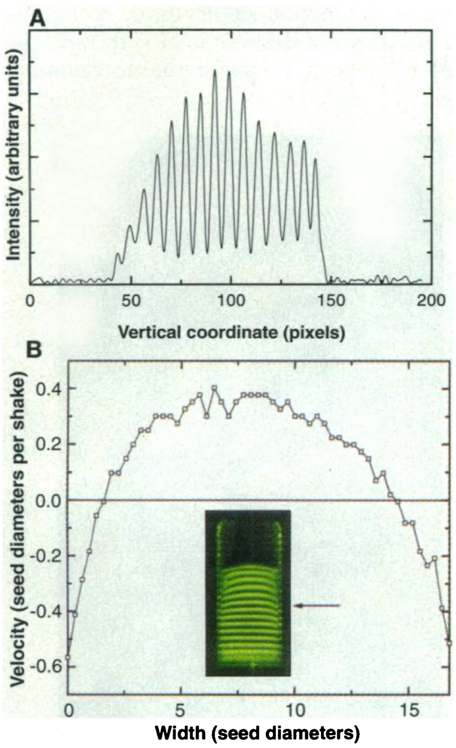

Fig. 3. Analysis of the stripe deformation seen in Fig. 2. (**A**) Vertical trace through the center of an image similar to that in Fig. 2B but shaken at $\Gamma = 4g$. The peaks seen in the graph are maxima in the nuclear magnetic resonance signal intensity and correspond to the position of the stripes in the image. The precise location of the maxima can be determined with an accuracy better than 0.1 seed diameters. (**B**) High-resolution velocity profile for the sixth stripe from the surface [assembled from many traces of the type shown in (A)]. The slight asymmetry in the plot is the result of residual, inadvertent deviations from true vertical motion during a shake. The horizontal scale encompasses the entire width of the cylinder; the total vertical scale corresponds to about 1 seed diameter. The zero velocity is determined by the position of the stripe in the single layer of seeds cemented to the container wall. Positive values of velocity correspond to upward motion of the seeds.

$$\frac{dj_d}{dz} = -\frac{j_d}{\xi} \quad (2)$$

Particle conservation requires $j_d(z) \propto j_u(z)$, so that

$$v_u \propto j_u \propto \exp(-z/\xi) \quad (3)$$

At depths $z > \xi$ the convection velocity becomes exponentially small; this finding provides a natural explanation for the existence of a "dead zone" reported in previous experiments near the bottom of the container (*6, 13*).

We have demonstrated the use of MRI as a noninvasive way to obtain quantitative information about convective flow in vibrated granular systems. The method enables direct measurement of the width of the boundary region that returns the convecting material to the lower part of the container. In addition, we have found an exponential depth dependence of the velocity of the material, which is consistent with a simple heuristic model of flow. The technique described here can be used to study other properties of granular media (*25, 26*); for example, because it enables tracking of individual seeds, it may be applicable to problems such as size separation (*13, 27, 28*) or compaction (*29, 30*). The granular flow studied here was cylindrically symmetric, so that cross sections (Figs. 2 and 3) contained all the relevant spatial information. Because MRI can be used to visualize arbitrary cross sections and to assemble them into a three-dimensional picture, our method can be extended to the analysis of nonsymmetric flows.

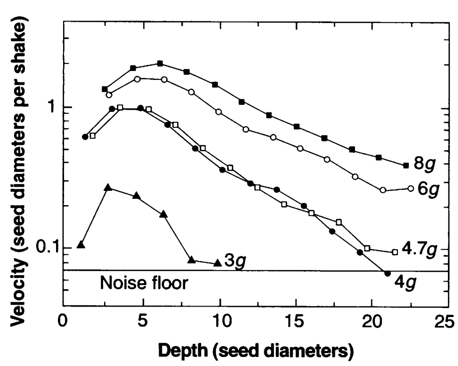

Fig. 4. The vertical velocity, v (displacement per shake), of the central region of each stripe as a function of depth, z, below the top surface. A straight line on this plot indicates an exponential depth dependence of the velocity. Data for five values of Γ (3 to $8g$) are plotted; the noise floor for the measurements is indicated by the horizontal line. The decrease in the vertical velocity component close to the top surface is expected, because the particle motion in this region possesses a significant horizontal component as seeds move from the central region toward the walls. At the uppermost surface, the vertical displacement after a shake is necessarily zero. This velocity roll-off at the surface was not detected by previous experimental methods but is made clear by the MRI method.

REFERENCES AND NOTES

1. M. Faraday, *Philos. Trans. R. Soc. London* **52**, 299 (1831).
2. B. J. Ennis, J. Green, R. Davis, *Chem. Eng. Prog.* **90**, 32 (April 1994).
3. S. B. Savage, *J. Fluid Mech.* **92**, 53 (1979).
4. C. S. Campbell, *Annu. Rev. Fluid Mech.* **22**, 57 (1990).
5. P. K. Haff, in *Granular Matter*, A. Mehta, Ed. (Springer-Verlag, New York, 1993), pp. 141–160.
6. Y.-H. Taguchi, *Phys. Rev. Lett.* **69**, 1367 (1992).
7. J. A. C. Gallas, H. J. Herrmann, S. Sokolowski, *ibid.*, p. 1371.
8. A. Rosato *et al.*, *ibid.* **58**, 1038 (1987).
9. R. Jullien *et al.*, *ibid.* **69**, 640 (1992).
10. H. Takahashi, A. Suzuki, T. Tanaka, *Powder Technol.* **2**, 65 (1968–69).
11. T. G. Drake, *J. Geophys. Res.* **95**, 8681 (1990).
12. E. Clement, J. Duran, J. Rajchenbach, *Phys. Rev. Lett.* **69**, 1189 (1992).
13. J. B. Knight *et al.*, *ibid.* **70**, 3728 (1993).
14. G. Radkai, *Powder Technol.* **15**, 187 (1976).
15. G. W. Baxter, R. P. Behringer, T. Fagert, G. A. Johnson, *Phys. Rev. Lett.* **62**, 2825 (1989).
16. C. F. Harwood, *Powder Technol.* **16**, 51 (1977).
17. S. A. Altobelli, R. C. Givler, E. Fukushima, *J. Rheol.* **35**, 721 (1991).
18. M. Nakagawa, S. A. Altobelli, A. Caprihan, E. Fukushima, E.-K. Jeong, *Exp. Fluids* **16**, 54 (1993).
19. C. Laroche, S. Douady, S. Fauve, *J. Phys. (France)* **50**, 699 (1989).
20. P. Evesque and J. Rajchenbach, *Phys. Rev. Lett.* **62**, 44 (1989).
21. H. K. Pak and R. P. Behringer, *ibid.* **71**, 1832 (1993).
22. L. Axel and L. Dougherty, *Radiology* **171**, 841 (1989).
23. To extract the precise center locations of the horizontal stripes from images such as in Fig. 2, we oversampled each vertical column of pixels in the image 10 times. This process—which involves Fourier transformations of each column and addition of zeros at high frequencies (zero filling) to yield a 10-fold increase in the number of points, followed by inverse Fourier transformations—allows us to extract the central locations of the stripes with 10 times the precision provided by the original image. Simulations of this technique with generated data, where stochastic noise was added with approximately the same amplitude as the noise in the actual data, indicate that our measurements of the center locations are accurate to within ± 0.3 pixel. This procedure sets the noise floor indicated in Fig. 4. The vertical displacement is then simply the difference in position of the stripe centers between the data after one shake and the control data.
24. E. E. Ehrichs *et al.*, in preparation.
25. H. M. Jaeger and S. R. Nagel, *Science* **255**, 1523 (1992).
26. S. R. Nagel, *Rev. Mod. Phys.* **64**, 321 (1992).
27. O. Zik, D. Levine, S. G. Lipson, S. Shtrikman, J. Stavans, *Phys. Rev. Lett.* **73**, 644 (1994).
28. K. M. Hill and J. Kakalios, *Phys. Rev. E* **49**, R3610 (1994).
29. G. C. Barker and A. Mehta, *ibid.* **47**, 184 (1993).
30. J. B. Knight, C. Fandrich, C. N. Lau, H. M. Jaeger, S. R. Nagel, *ibid.*, in press.
31. A. Kumar *et al.*, *J. Magn. Reson.* **18**, 69 (1975).

32. We are grateful to D. Levine for pointing out reference 17 to us and discussing the possibility of MRI of particles, and to M. J. Lipton for his support. Data were taken at the University of Illinois at Chicago MRI Center. Supported in part by U.S. Department of Energy grant DE-FG02-92ER25119 and by the Materials Research Laboratory at the University of Chicago under NSF grant DMR-MRL 88-19860. E.E.E. received fellowship support from the Grainger Foundation. J.B.K. was supported by an NSF Graduate Student Fellowship. H.M.J. thanks the David and Lucile Packard Foundation and the Alfred P. Sloan Foundation for fellowship support.

26 September 1994; accepted 23 January 1995